Oxidative Additions and Luminescence Involving IrAuIr Chains Formed by Binding of Gold(I) to the Metallamacrocycle $Ir_2Cl_2(CO)_2[\mu\text{-}Ph_2PCH_2As(Ph)CH_2PPh_2]_2$

Alan L. Balch,* Jeffrey K. Nagle, Douglas E. Oram, and Philip E. Reedy, Jr.

Contribution from the Department of Chemistry, University of California, Davis, California 95616. *Received June 22, 1987*

Abstract: Treatment of $Ir_2Cl_2(CO)_2(\mu\text{-dpma})_2$ (dpma = bis(diphenylphosphino)methylphenylarsine) with ClAu(CO) in dichloromethane yields red-violet $[Ir_2AuCl_2(CO)_2(\mu\text{-dpma})_2]Cl$ while the corresponding reaction with $AuCl_4^-$ gives $[Ir_2AuCl_4(CO)_2(\mu\text{-dpma})_2]^+$. Oxidation of $[Ir_2AuCl_2(CO)_2(\mu\text{-dpma})_2]^+$ to $[Ir_2AuCl_4(CO)_2(\mu\text{-dpma})_2]^+$ can be affected by ClAu(CO), dichlorine, carbon tetrachloride, or chloroform with irradiation with visible light. The chloride ligands in these complexes have been exchanged to give the corresponding bromo and iodo complexes. The preparation of some mixed-halide species are also described. At low temperature, these produce predominantly one isomeric complex. The structures of $[Ir_2AuCl_2(CO)_2(\mu\text{-dpma})_2]BPh_4$ and $[Ir_2AuCl_4(CO)_2(\mu\text{-dpma})_2]Cl$ have been determined by X-ray crystallography. The first contains a bent chain (Ir–Au–Ir angle, 149.0 (1)°) with nearly equivalent Ir–Au separations (3.059 (1), 3.012 (1) Å), planar $Ir(CO)ClP_2$ units, and a linear As–Au–As unit at the center. $[Ir_2AuCl_4(CO)_2(\mu\text{-dpma})_2]^+$ contains a nearly linear chain (Ir–Au–Ir angle, 173.1 (1)°) with shorter Ir–Au distances (2.812 (2), 2.806 (2) Å). The iridium ions are six-coordinate with $P_2Cl_2(CO)Au$ coordination, while the central gold has planar As_2Ir_2 coordination. The electronic spectra of these complexes are dominated by intense absorption features in the visible, which are analyzed in terms of a qualitative molecular orbital scheme as involving delocalized d → p transitions. The reduced species, $[Ir_2AuX_2(CO)_2(\mu\text{-dpma})_2]^+$, show intense luminescence in solution at 25 °C attributed to fluorescence. The photochemical behavior of these compounds is discussed in the context of the excited-state electronic structure.

The novel chemical and spectroscopic features of binuclear d^8 complexes including examples with bridging diphosphine,[1] diphosphite,[2] diisocyanide,[3] and pyrazolate[4] bridges have received considerable experimental study. In a few cases, it has been possible to examine related trinuclear d^8 systems. Some aspects of the chemistry of $Rh_3(CNR)_{12}^{3+}$ are known, but ready dissociation of a $Rh(CNR)_4^+$ unit greatly limits observations of this system.[5,6] The phosphine-bridged complexes **1**[7,8] and **2**[9] offer

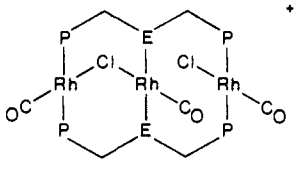

1a, E = P
b, E = As

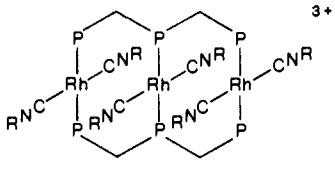

2

examples in which such dissociation is limited by the presence of a firmly bound bridging triphosphine. The electronic structures of these trinuclear species are dominated by the overlap of the out-of-plane filled d_{z^2} and empty p_z orbitals on each planar rhodium ion (with the z axis collinear with the Rh_3 chain).

Scheme I

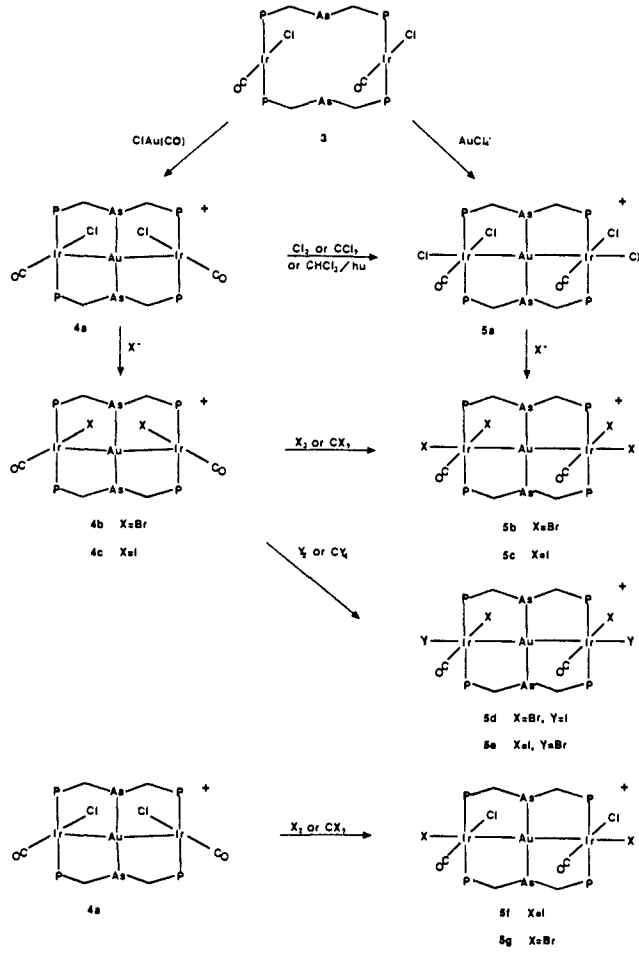

The availability of the metallamacrocycles $Ir_2Cl_2(CO)_2(\mu\text{-dpma})_2$ (**3**; dpma = bis(diphenylphosphino)methylphenylarsine) and its rhodium analogue make it possible to prepare and examine the properties of nearly linear trinuclear chains with metal ions

(1) Balch, A. L. In *Homogeneous Catalysis with Metal Phosphine Complexes*; Pignolet, L. H., Ed.; Plenum: New York, 1983; p 167.
(2) Che, C.-M.; Butler, L. G.; Gray, H. B. *J. Am. Chem. Soc.* **1981**, *103*, 7796. Fordyce, W. A.; Brummer, J. G.; Crosby, G. A. *J. Am. Chem. Soc.* **1981**, *103*, 7061. Roundhill, D. M. *J. Am. Chem. Soc.* **1985**, *107*, 4354.
(3) Miskowski, N. M.; Nobinger, G. L.; Kliger, D. S.; Hammond, G. S.; Lewis, N. S.; Mann, K. R.; Gray, H. B. *J. Am. Chem. Soc.* **1978**, *100*, 485. Rice, S. F.; Gray, H. B. *J. Am. Chem. Soc.* **1981**, *103*, 1593. Rice, S. F.; Milder, S. J.; Gray, H. B. *Coord. Chem. Rev.* **1982**, 394. Mann, K. R.; Thich, J. A.; Bell, R. A.; Coyle, C. L.; Gray, H. B. *Inorg. Chem.* **1980**, *19*, 2426. Mann, K. R.; Bell, R. A.; Gray, H. B. *Inorg. Chem.* **1979**, *18*, 2671.
(4) Marshall, J. L.; Stobart, S. R.; Gray, H. B. *J. Am. Chem. Soc.* **1984**, *106*, 3027. Caspar, J. V.; Gray, H. B. *J. Am. Chem. Soc.* **1984**, *106*, 3029.
(5) Mann, K. R.; Lewis, N. S.; Willaims, R. M.; Gray, H. B.; Gordon, J. G., II *Inorg. Chem.* **1978**, *17*, 829.
(6) Balch, A. L.; Olmstead, M. M. *J. Am. Chem. Soc.* **1979**, *101*, 3128.
(7) Balch, A. L.; Fossett, L. A.; Guimerans, R. R.; Olmstead, M. M.; Reedy, P. E., Jr.; Wood, F. E. *Inorg. Chem.* **1986**, *25*, 1248.
(8) Balch, A. L.; Fossett, L. A.; Olmstead, M. M.; Reedy, P. E., Jr. *Organometallics* **1986**, *5*, 1929.
(9) Balch, A. L.; Fossett, L. A.; Nagle, J. K.; Olmstead, M. M., unpublished results.

0002-7863/88/1510-0454$01.50/0

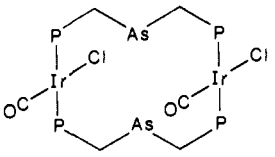

3

with different electronic structure occupying the central position.[7,8,10,11] Here we describe the formation of $d^8d^{10}d^8$ chains obtained by introducing gold(I) into 3. The physical characteristics, particularly the electronic spectra of these new IrAuIr chains, are reported, and their chemical behavior in oxidative addition reactions is described. Related work on the three-fragment, two-centered oxidative addition of $AuCl_4^-$ to 3 has been reported briefly.[13]

Results

Synthetic Studies. The reaction chemistry is summarized in Scheme I. Treatment of the metallamacrocycle $Ir_2(CO)_2Cl_2(\mu\text{-dpma})_2$ with ClAu(CO) in dichloromethane solution at −60 °C produces a deep red-violet solution from which crystals of $[Ir_2AuCl_2(CO)_2(\mu\text{-dpma})_2]Cl$ (**4a**) are obtained by the addition of diethyl ether. Spectroscopic data for this and other new compounds are given in Table I. The new complex is readily identified by its single ^{31}P NMR resonance, which is distinct from that of $Ir_2(CO)_2Cl_2(\mu\text{-dpma})_2$. The infrared spectrum shows carbonyl stretching absorptions at 1963 and 1952 cm^{-1}, which are in the region characteristic of Ir(I) compounds.[13] The analogous rhodium complex, $[Rh_2AuCl_2(CO)_2(\mu\text{-dpma})_2]^+$ (**6**), was prepared by the reaction of $Rh_2Cl_2(CO)_2(\mu\text{-dpma})_2$ with ClAu(CO) and isolated as the chloride salt by the addition of diethyl ether.

The reaction between $Ir_2(CO)_2(\mu\text{-dpma})_2$ and $AuCl_4^-$ results in a three-fragment, two-center oxidative addition.[12] The product, $[Ir_2AuCl_4(CO)_2(\mu\text{-dpma})_2]Cl$ (**5a**), is obtained as a red-violet crystalline solid after the addition of diethyl ether. Its spectroscopic properties (Table I) clearly differentiate it from the starting metallamacrocycle and its Au(I) addition product, $[Ir_2AuCl_2(CO)_2(\mu\text{-dpma})_2]^+$ (**4a**). The infrared spectrum indicates that the iridium centers have been oxidized: the carbonyl stretching vibration occurs at 2011 cm^{-1}. $[Ir_2AuCl_4(CO)_2(\mu\text{-dpma})_2]^+$ (**5a**) is also formed when $Ir_2Cl_2(CO)_2(\mu\text{-dpma})_2$ or $[Ir_2AuCl_2(CO)_2(\mu\text{-dpma})_2]^+$ (**4a**) is treated with an excess of ClAu(OC). In this case, ClAu(OC) acts as the oxidizing agent and a deposit of gold, generally as a mirror, forms during the reaction. Because of the oxidizing ability of ClAu(OC), it is essential to carry out the preparation of the gold(I) adduct, $[Ir_2AuCl_2(CO)_2(\mu\text{-dpma})_2]^+$ (**4a**), at low temperature; at higher temperatures the product is contaminated with some $[Ir_2AuCl_4(CO)_2(\mu\text{-dpma})_2]^+$.

$[Ir_2AuCl_2(CO)_2(\mu\text{-dpma})_2]^+$ (**4a**) is readily converted into $[Ir_2AuCl_4(CO)_2(\mu\text{-dpma})_2]^+$ (**5a**) in other ways. Addition of a dichloromethane solution of dichlorine to **4a** produces this oxidation. Treatment of **4a** with carbon tetrachloride also yields **5a**. In the dark, this reaction was nearly complete in 5 h, but when irradiated with visible light ($\lambda > 440$ nm), the oxidation, under otherwise comparable conditions, was complete in under 30 min. The ^{31}P NMR spectrum indicated that **5a** was the sole product; no isomers of **5a** were present. The oxidation of **4a** to **5a** with chloroform is significantly slower than the reaction with carbon tetrachloride. The ^{31}P NMR spectrum of a sample of **4a** in chloroform showed no change after storage for 3 days in the absence of light. However, a corresponding sample, irradiated with visible light for 3 h, showed 50% conversion to **5a**. Further irradiation resulted in the complete conversion of **4a** into **5a** as monitored by ^{31}P NMR spectroscopy. At this point, two other resonances at 25.3 and −13.9 ppm appeared in the ^{31}P NMR spectrum with intensities 19% and 18% of that of **5a**. These may be due to isomers of **5a**. No reaction between **4a** and dichloromethane was observed even after 24 h of photolysis.

The structures of both **4a** and **5a** have been determined unambiguously, and it is clear from our observations that our procedures give **5a** in a high degree of isomeric purity. If we assume that the $Ir_2Au(\mu\text{-dpma})_2$ core remains intact and has C_s symmetry (which it does not), then there are four isomeric arrangements of the chloride and carbon monoxide ligands so long as one carbon monoxide remains bound to each iridium. These include **5a** (with cis carbon monoxide ligands, a corresponding isomer with trans carbonyl groups, an isomer with one carbon monoxide in an axial position trans to an Ir–Au bond, and an isomer with both carbon monoxide in axial sites). We consider that the predominant formation of isomer **5a** as established here is conserved throughout the other related chemical transformations seen in Scheme I and that the carbon monoxide ligands will retain the relative cis orientation.

Because the structures of some related trinuclear rhodium complexes are strongly dependent on the particular halide ligands present,[7] and because we wanted to probe the effect of halide ligands on the electronic spectra (vide infra), the exchange of halide ligands via metathesis reactions was examined. Treatment of dichloromethane solutions of $[Ir_2AuCl_2(CO)_2(\mu\text{-dpma})_2]^+$ (**4a**) with methanol solutions of sodium bromide or sodium iodide results in rapid halide exchange and the formation of the corresponding $[Ir_2AuX_2(CO)_2(\mu\text{-dpma})_2]^+$ (X = Br (**4b**), I (**4c**)). The spectroscopic data indicate that no structural change occurred upon this substitution.

Oxidation of $[Ir_2AuBr_2(CO)_2(\mu\text{-dpma})_2]^+$ (**4b**) with bromine or carbon tetrabromide yields $[Ir_2AuBr_4(CO)_2(\mu\text{-dpma})_2]^+$ (**5b**). The reaction of **4b** with carbon tetrabromide proceeds cleanly and requires only 1 mol of carbon tetrabromide/mol of **4b**. The oxidation with dibromine is not quite as clean; other compounds are detected spectroscopically in minor amounts. Metathesis of $[Ir_2AuCl_4(CO)_2(\mu\text{-dpma})_2]^+$ (**5a**) with sodium bromide yields **5b**, which has been isolated as the bromide salt. However, when the conversion of this only very slightly soluble salt into the corresponding tetraphenylborate salt was attempted using methanolic sodium tetraphenylborate, significant decomposition to several unidentified products occurred. Thus, the best route to **5b** is oxidation with carbon tetrabromide.

Similar oxidative and metathetical routes to $[Ir_2AuI_4(CO)_2(\mu\text{-dpma})_2]BPh_4$ (**5c**) have been devised. Treatment of $[Ir_2AuI_2(CO)_2(\mu\text{-dpma})_2]BPh_4$ (**4c**) with 1 equiv of diiodine or carbon tetraiodide produces **5c**, which has been isolated in good yield. The metathesis of $[Ir_2AuCl_4(CO)_2(\mu\text{-dpma})_2]^+$ (**5a**) with methanolic sodium iodide also yields **5c**; however, significant amounts of the reduced complex, **4c**, are also observed in both the infrared and ^{31}P spectra. Apparently, methanol is acting as a reducing agent in the reaction.

To evaluate the specificity of the oxidation reactions and to further study the effects of varying the halide ligands on the electronic and ^{31}P NMR spectra, four mixed-halide complexes of the general formula $[Ir_2AuX_2Y_2(CO)_2(\mu\text{-dpma})_2]^+$ (X, Y = Cl, Br, I) were synthesized. In order to minimize scrambling of halide ligands through interionic exchange,[14] these reactions were conducted at low temperature (−60 °C) and the products were identified spectroscopically.

Treatment of $[Ir_2AuBr_2(CO)_2(\mu\text{-dpma})_2]^+$ (**4b**) with diiodine in chloroform produced a deep blue solution showing by ^{31}P NMR a major singlet at −22.0 ppm and two other singlets at −11.1 and −15.8 ppm in a 100:14:12 intensity ratio. A similar reaction with carbon tetraiodide produced identical spectroscopic results. The predominant resonance is assigned to an isomer (isomer I) of $[Ir_2AuBr_2I_2(CO)_2(\mu\text{-dpma})_2]^+$ with equivalent iridium environments while the two other peaks are believed to be caused by a second isomer (isomer II) with inequivalent iridium environments. Addition of 1 equiv of dibromine to a solution of $[Ir_2AuI_2(CO)_2(\mu\text{-dpma})_2]^+$ produces a deep blue solution whose ^{31}P NMR

(10) Balch, A. L.; Fossett, L. A.; Olmstead, M. M.; Oram, D. E.; Reedy, P. E., Jr. *J. Am. Chem. Soc.* **1985**, *107*, 5272.
(11) Balch, A. L.; Ghedini, M.; Oram, D. E.; Reedy, P. E., Jr. *Inorg. Chem.* **1987**, *26*, 1223.
(12) Balch, A. L.; Oram, D. E.; Reedy, P. E., Jr. *Inorg. Chem.* **1987**, *26*, 1836.
(13) Vaska, L. *Acc. Chem. Res.* **1968**, *1*, 335.
(14) Hunt, C. T.; Balch, A. L. *Inorg. Chem.* **1982**, *21*, 1641.

Table I. Infrared, ^{31}P NMR, and Electronic Spectral Data

compound	^{31}P NMR:[b] δ	UV–vis: λ_{max}, nm (ϵ, $M^{-1}\cdot cm^{-1}$)[b]	IR:[a] ν(CO), cm^{-1}	emission: λ_{max}, nm
$Ir_2Cl_2(CO)_2(\mu\text{-dpma})_2$ (**3**)	18.6	432 (1900), 383 (16 000)	1974, 1964	
$[Ir_2AuCl_2(CO)_2(\mu\text{-dpma})_2]BPh_4$ (**4a**)	15.1	508 (32 000), 412 (3500), 357 (5400), 328 (9000), 296 (10 500)	1968, 1953	606
$[Ir_2AuBr_2(CO)_2(\mu\text{-dpma})_2]BPh_4$ (**4b**)	12.2	518 (39 000), 416 (3600), 369 (5200), 333 (9500), 303 (10 500)	1968, 1957	614
$[Ir_2AuI_2(CO)_2(\mu\text{-dpma})]BPh_4$ (**4c**)	7.0	536 (35 000), 424 (4200), 367 (5200), 342 (9400)	1971, 1953	624
$[Ir_2AuCl_4(CO)_2(\mu\text{-dpma})_2]Cl$ (**5a**)	−8.4 (−7.2, $CDCl_3$)	520 (29 000), 446 (3200), 365 (4100)	2011	
$[Ir_2AuBr_4(CO)_2(\mu\text{-dpma})_2]BPh_4$ (**5b**)	−21.2	556 (32 000), 484 (5200), 399 (3200)	2018, 2004	
$[Ir_2AuI_4(CO)_2(\mu\text{-dpma})_2]BPh_4$ (**5c**)	−36.4	662 (44 000), 424 (14 200), 642 (16 300)	2022, 2012	
$[Ir_2AuBr_2I_2(CO)_2(\mu\text{-dpma})_2]BPh_4$ (**5d**)	−22.0[c]	614		
$[Ir_2AuBr_2I_2(CO)_2(\mu\text{-dpma})_2]BPh_4$ (**5e**)	−31.2[c]	610		
$[Ir_2AuCl_2I_2(CO)_2(\mu\text{-dpma})_2]BPh_4$ (**5f**)	−10.6[c]	580		
$[Ir_2AuBr_2Cl_2(CO)_2(\mu\text{-dpma})_2]BPh_4$ (**5g**)	−7.0[c]	542		
$[Rh_2AuCl_2(CO)_2(\mu\text{-dpma})_2]BPh_4$ (**6**)	24.3	472 (21 000), 395 (1600)	1974, 1964	

[a] Recorded as mineral oil mulls. [b] Recorded in dichloromethane. [c] Recorded in chloroform at −50 °C. [d] $^1J(Rh,P)$ = 122.9 Hz.

spectrum shows only a single peak at −31.2 ppm. This is assigned as a third isomer (isomer III) of $[Ir_2AuBr_2I_2(CO)_2(\mu\text{-dpma})_2]^+$ which must have a symmetrical structure with equivalent iridium environments. Four isomeric structures are possible for $[Ir_2AuI_2Br_2(CO)_2(\mu\text{-dpma})_2]^+$. Two of these, **5d** and **5e** (see Scheme I), are symmetrical. The other two, **5h** and **5i**, are unsymmetrical. Consequently, isomers I and III may have structures **5d** and **5e**, while II can have structure **5h** or **5i**. On the basis of the observation of a number of examples of diaxial oxidative addition,[6,9] we expect that these additions occur preferentially at the vacant axial sites and so we assign structure **5d** to isomer I and structure **5e** to isomer III. Since we expect it to be difficult to transfer halide from one iridium to another during the oxidation, we believe it is more likely that isomer II has structure **5h** rather than **5i**. When solutions of these isomers of $[Ir_2AuBr_2I_2(CO)_2(\mu\text{-dpma})_2]^+$ are warmed to room temperature, new peaks develop in the ^{31}P NMR spectrum. We interpret these changes to interionic halide ligand scrambling.

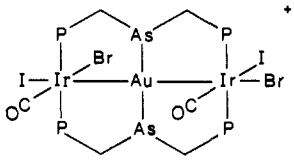

5h

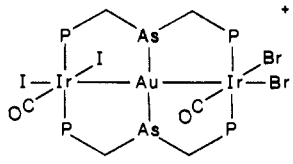

5i

Addition of 1 equiv of diiodine to $[Ir_2AuCl_2(CO)_2(\mu\text{-dpma})_2]^+$ (**4a**) gives a deep blue solution whose ^{31}P NMR spectrum shows a major resonance at −10.6 ppm and four minor resonances of −4.5, −11.4, −22.6, and −24.9 ppm, with relative intensities of 100:8.3:12.3:5.0:5.9, respectively. The major resonance is assigned to a symmetrical isomer of $[Ir_2AuCl_2I_2(CO)_2(\mu\text{-dpma})_2]^+$, with structure **5f** considered the most likely. The reaction of **4a** with carbon tetraiodide gives a similar solution with identical spectroscopic features.

A mixed chloride/bromide complex was prepared by the reaction of carbon tetrabromide with $[Ir_2AuCl_2(CO)_2(\mu\text{-dpma})_2]^+$ (**4a**) in a 1:1 molar ratio. The ^{31}P NMR spectrum of the resulting purple solution shows a major resonance at −7.2 ppm and a minor one at −5.0 ppm in a ratio of 100:26. We assign the major resonance to the symmetrical isomer with structure **5g**, although the data are equally compatable with structure **5j**.

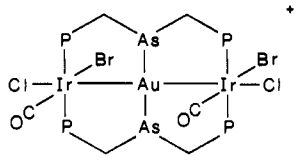

5j

Crystal and Molecular Structure of $[Ir_2AuCl_2(CO)_2(\mu\text{-dpma})_2]BPh_4\cdot CH_2Cl_2$. The solid contains the cation, $[Ir_2AuCl_2(CO)_2(\mu\text{-dpma})_2]^+$, a tetraphenylborate, and one dichloromethane molecule in the asymmetric unit. There are no unusual contacts between these constituents. Atomic positional parameters are given in Table II. Selected interatomic distances and angles are compiled in Tables III and IV, respectively. A perspective drawing of the cation is presented in Figure 1. Although the cation has no crystallographically imposed symmetry, it does approximate C_2 symmetry, with the twofold rotation axis bisecting the As–Au–As and Ir···Au···Ir angles. Normal molecular motion in solution increases the effective symmetry to C_{2v} and renders all four phosphorus atoms equivalent.

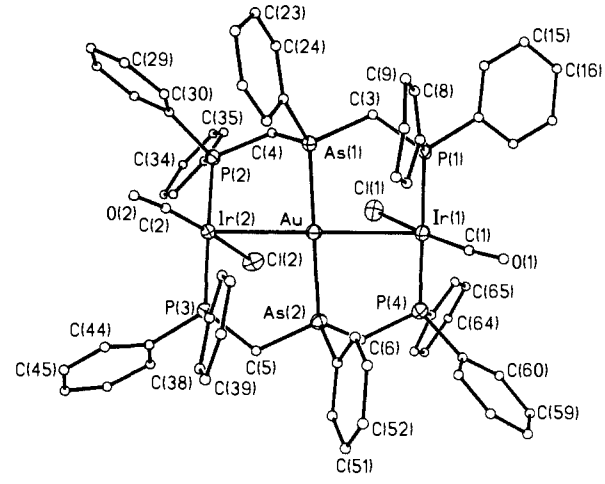

Figure 1. Perspective drawing of $[Ir_2AuCl_2(CO)_2(\mu\text{-dpma})_2]^+$ (**4a**) using 50% thermal contours for anisotropically refined atoms and uniform arbitrarily sized circles for carbon atoms.

The structure shows that the gold(I) ion is bound at the center of the metallamacrocycle with essentially linear coordination of the gold(I) by the two arsenic donors, with an As–Au–As angle of 173.9 (1)°. The As–Au distances (2.397, 2.396 Å) are similar to that in $Ph_3AsAuBr$ (2.342 (5) Å).[15] The Ir···Au separations (3.012, 3.059 Å) are rather long and are outside the range (2.59–2.72 Å) found for unbridged Ir–Au bonds.[16-20] These metal–metal separations are, however, shorter than those found in the $d^8d^8d^8$ chain in $[Rh_2Ir(CO)_3(\mu\text{-Cl})Cl(\mu\text{-dpma})_2]^+$ (Rh···Ir, 3.188, 3.154).[8] The Ir···Au···Ir chain is bent with an angle of 149.0°. This is similar to the situation in $[Rh_2Ir(CO)_3(\mu\text{-Cl})$-

(15) Einstein, F. W. B.; Restivo, R. *Acta Crystallogr., Sect. B: Struct. Crystallogr. Cryst. Chem.* **1975**, *B31*, 624.
(16) Casalnuova, A. L.; Pignolet, L. H.; van der Velden, J. W. A.; Bour, J. J.; Steggerda, J. J. *J. Am. Chem. Soc.* **1983**, *105*, 5957.
(17) Casalnuova, A. L.; Laska, T.; Nilsson, P. V.; Olofson, J.; Pignolet, L. H. *Inorg. Chem.* **1985**, *24*, 233.
(18) Casalnuovo, A. L.; Casalnuovo, J. A.; Nilsson, P. V.; Pignolet, L. H. *Inorg. Chem.* **1985**, *24*, 2554.
(19) Casalnuovo, A. L.; Laska, T.; Nilsson, P. V.; Olofson, J.; Pignolet, L. H.; Bos, W.; Bour, J. J.; Steggerda, J. J. *Inorg. Chem.* **1985**, *24*, 182.
(20) Nicholls, J. N.; Raithby, P. R.; Vargas, M. D. *J. Chem. Soc., Chem. Commun.* **1986**, 1617.

Table II. Atomic Coordinates ($\times 10^4$) and Isotropic Thermal Parameters ($Å^2 \times 10^3$) for $[Ir_2AuCl_2(CO)_2(\mu\text{-dpma})_2]BPh_4 \cdot CH_2Cl_2$

	x	y	z	U[a]		x	y	z	U[a]
Ir(1)	1669 (1)	8582 (1)	8627 (1)	20 (1)*	C(39)	3257 (12)	5581 (7)	7206 (6)	37 (4)
Ir(2)	1317 (1)	6040 (1)	9076 (1)	17 (1)*	C(40)	4148 (13)	5791 (7)	7455 (6)	42 (4)
Au	2022 (1)	7240 (1)	8743 (1)	18 (1)*	C(41)	4135 (12)	5998 (7)	7941 (5)	33 (4)
P(1)	2899 (3)	8672 (2)	9253 (1)	19 (1)*	C(42)	3247 (10)	5980 (6)	8182 (5)	24 (3)
P(2)	1323 (3)	6276 (2)	9909 (1)	19 (1)*	C(43)	612 (10)	5109 (6)	8090 (5)	20 (3)
P(3)	1238 (3)	5820 (2)	8240 (1)	19 (1)*	C(44)	1188 (12)	4584 (7)	8048 (5)	30 (3)
P(4)	424 (3)	8479 (2)	8022 (1)	24 (1)*	C(45)	683 (13)	4072 (8)	7967 (6)	41 (4)
As(1)	2635 (1)	7366 (1)	9581 (1)	20 (1)*	C(46)	−287 (13)	4033 (8)	7912 (6)	40 (4)
As(2)	1240 (1)	7130 (1)	7937 (1)	19 (1)*	C(47)	−847 (13)	4544 (7)	7971 (6)	38 (4)
Cl(1)	576 (3)	8215 (2)	9196 (1)	31 (1)*	C(48)	−396 (11)	5101 (7)	8056 (5)	29 (3)
Cl(2)	−118 (3)	6618 (2)	8966 (1)	29 (1)*	C(49)	1994 (11)	7153 (6)	7358 (5)	22 (3)
O(1)	2925 (10)	9236 (6)	7971 (5)	54 (3)	C(50)	1628 (12)	7000 (6)	6900 (5)	28 (3)
O(2)	2963 (8)	5183 (5)	9207 (4)	37 (3)	C(51)	2180 (14)	7012 (8)	6492 (7)	45 (4)
Cl(3)	1244 (9)	1932 (5)	−173 (4)	48 (3)	C(52)	3182 (14)	7157 (8)	6564 (7)	49 (5)
Cl(4)	2355 (9)	2905 (5)	443 (4)	44 (3)	C(53)	3592 (13)	7298 (7)	7027 (6)	39 (4)
B	2747 (13)	8500 (8)	1650 (6)	27 (4)	C(54)	2998 (12)	7312 (7)	7418 (6)	35 (4)
C(1)	2438 (12)	8957 (7)	8209 (6)	35 (4)	C(55)	616 (10)	8820 (6)	7415 (5)	23 (3)
C(2)	2354 (10)	5540 (6)	9166 (5)	23 (3)	C(56)	1361 (11)	8597 (7)	7131 (5)	31 (3)
C(3)	2695 (10)	8202 (6)	9790 (5)	21 (3)	C(57)	1496 (12)	8827 (7)	6678 (5)	33 (4)
C(4)	1719 (11)	7042 (6)	10043 (5)	21 (3)	C(58)	905 (13)	9295 (8)	6495 (6)	43 (4)
C(5)	546 (10)	6367 (6)	7856 (5)	23 (3)	C(59)	239 (12)	9513 (7)	6776 (6)	37 (4)
C(6)	167 (10)	7697 (5)	7860 (5)	19 (3)	C(60)	76 (11)	9300 (6)	7241 (5)	27 (3)
C(7)	4122 (11)	8452 (7)	9082 (5)	32 (4)	C(61)	−779 (11)	8795 (6)	8169 (5)	25 (3)
C(8)	4880 (18)	8403 (12)	9411 (10)	85 (8)	C(62)	−1626 (12)	8564 (7)	7921 (6)	36 (4)
C(9)	5800 (19)	8189 (11)	9299 (9)	82 (7)	C(63)	−2507 (15)	8823 (8)	8029 (7)	52 (5)
C(10)	5906 (22)	8015 (12)	8779 (10)	97 (9)	C(64)	−2548 (18)	9281 (10)	8394 (8)	73 (7)
C(11)	5088 (18)	7920 (10)	8510 (9)	73 (7)	C(65)	−1669 (15)	9490 (10)	8591 (7)	61 (6)
C(12)	4186 (14)	8163 (8)	8635 (7)	46 (4)	C(66)	−828 (14)	9225 (8)	8507 (6)	44 (4)
C(13)	2990 (10)	9421 (6)	9513 (5)	20 (3)	C(67)	3747 (11)	8854 (6)	1522 (5)	24 (3)
C(14)	3588 (11)	9551 (6)	9932 (5)	25 (3)	C(68)	4099 (10)	9345 (6)	1801 (5)	23 (3)
C(15)	3585 (12)	10125 (7)	10143 (6)	35 (4)	C(69)	4914 (11)	9694 (7)	1688 (5)	33 (4)
C(16)	3004 (12)	10563 (7)	9938 (6)	36 (4)	C(70)	5449 (14)	9500 (8)	1285 (6)	49 (5)
C(17)	2374 (12)	10441 (7)	9513 (6)	37 (4)	C(71)	5149 (12)	9026 (7)	1014 (6)	36 (4)
C(18)	2391 (11)	9866 (7)	9306 (5)	30 (3)	C(72)	4312 (10)	8712 (6)	1124 (5)	23 (3)
C(19)	3902 (10)	7043 (6)	9781 (5)	19 (3)	C(73)	2517 (11)	8582 (6)	2234 (5)	27 (3)
C(20)	4429 (12)	6744 (7)	9430 (6)	34 (4)	C(74)	2093 (11)	9104 (7)	2418 (5)	26 (3)
C(21)	5330 (13)	6480 (8)	9589 (6)	41 (4)	C(75)	1977 (11)	9186 (7)	2916 (5)	28 (3)
C(22)	5675 (17)	6508 (10)	10073 (8)	66 (6)	C(76)	2240 (11)	8729 (6)	3251 (5)	28 (3)
C(23)	5108 (13)	6822 (8)	10414 (7)	46 (4)	C(77)	2647 (12)	8237 (7)	3078 (6)	37 (4)
C(24)	4261 (12)	7057 (7)	10274 (6)	35 (4)	C(78)	2759 (11)	8147 (7)	2587 (5)	28 (3)
C(25)	2057 (10)	5803 (6)	10319 (4)	16 (3)	C(79)	2850 (11)	7785 (6)	1531 (5)	23 (3)
C(26)	1645 (10)	5430 (6)	10678 (4)	21 (3)	C(80)	3737 (11)	7497 (6)	1603 (5)	24 (3)
C(27)	2208 (12)	5018 (7)	10944 (5)	34 (4)	C(81)	3852 (13)	6858 (7)	1560 (6)	36 (4)
C(28)	3199 (11)	4961 (7)	10864 (5)	28 (3)	C(82)	3006 (11)	6517 (7)	1452 (5)	30 (3)
C(29)	3601 (11)	5315 (6)	10517 (5)	27 (3)	C(83)	2140 (12)	6795 (7)	1393 (6)	38 (4)
C(30)	3062 (11)	5736 (7)	10254 (5)	29 (3)	C(84)	2033 (11)	7415 (6)	1429 (5)	27 (3)
C(31)	148 (10)	6236 (6)	10176 (5)	21 (3)	C(85)	1827 (11)	8781 (6)	1294 (5)	23 (3)
C(32)	−550 (11)	5793 (6)	10001 (5)	27 (3)	C(86)	1954 (12)	9024 (7)	832 (5)	32 (4)
C(33)	−1403 (11)	5704 (7)	10216 (5)	26 (3)	C(87)	1202 (12)	9261 (7)	525 (6)	35 (4)
C(34)	−1633 (13)	6045 (7)	10623 (6)	41 (4)	C(88)	263 (14)	9227 (8)	663 (6)	45 (4)
C(35)	−988 (11)	6504 (7)	10793 (5)	29 (3)	C(89)	107 (13)	8975 (7)	1122 (6)	36 (4)
C(36)	−103 (11)	6586 (7)	10562 (5)	29 (3)	C(90)	848 (11)	8753 (6)	1414 (5)	28 (3)
C(37)	2390 (11)	5790 (6)	7948 (5)	25 (3)	C(91)	1412 (20)	2354 (11)	306 (9)	82 (7)
C(38)	2408 (12)	5579 (7)	7459 (5)	32 (4)					

[a] Values denoted by asterisks indicate equivalent isotropic U defined as one-third of the trace of the orthogonalized U_{ij} tensor.

$Cl(\mu\text{-dpma})_2]^+$ where the Rh···Ir···Rh angle is 156.3 (1)°.[8]

The two iridium(I) ions have planar $P_2(CO)Cl$ coordination. Comparison of the geometry of these units with those of other compounds containing $IrP_2(CO)Cl$ units, including $Ir(CO)Cl[(t\text{-Bu})_2P(CH_2)_{10}P(t\text{-Bu})_2]$,[21] $Ir(CO)Cl[P(o\text{-tol})_3]_2$,[22] and $Ir_2(CO)_2Cl_2(\mu\text{-}Ph_2P(CH_2)_3PPh_2)_2$,[23] reveals that the presence of the gold(I) produces no major structural change within the $IrP_2(CO)Cl$ unit. The phosphine ligands maintain the trans orientation that was present in the parent metallamacrocycle **1**, and the P–Ir–P units are nearly linear (angles of 178.4 and 177.3 (1)°).

There is a pronounced twist in the orientations of the coordination environment of the three metal ions. This is best seen by examining the dihedral angles presented in Table V. The average P–Ir–Au–As dihedral angle is 23°. As a result of this twisting, the two $Ir(CO)ClP_2$ units have a staggered (rather than eclipsed) relationship with an average P–Ir–Ir–P dihedral angle of 45.5°. The twisting also causes the plane of the $Ir(1)(CO)ClP_2$ group plane to be tilted so that it intersects the plane of the $Ir(2)(CO)ClP_2$ group at an angle of 65.1°. As a result of this tilting, the chloride ligands, Cl(1) and Cl(2), approach one another; but the resulting C(1)···Cl(2) distance, 3.748 Å, is greater than the sum of the van der Waals radii for two chlorine atoms (3.2 Å). Shorter contact between these two atoms has been alleviated by the twisting of the coordination planes of the two iridium centers.

It is informative to compare the structure of $[Ir_2AuCl_2(CO)_2(\mu\text{-dpma})_2]^+$ with the structures of $Ir_2AgCl_3(CO)_2(\mu\text{-dpma})_2$[24] and $Rh_2AgCl_3(CO)_2(\mu\text{-dpma})_2$.[11] These latter complexes have similar structures, **7**, in which a $d^8d^{10}d^8$ chain is involved.

(21) March, F. C.; Mason, R.; Thomas, K. M.; Shaw, B. L. *J. Chem. Soc., Chem. Commun.* **1975**, 584.
(22) Brady, R.; DeCamp, W. H.; Flynn, B. R.; Schneider, M. L.; Scott, J. D.; Vaska, L.; Werneke, M. L. *Inorg. Chem.* **1975**, *14*, 2669.
(23) Wang, H.-H.; Pignolet, L. H.; Reedy, P. E., Jr.; Olmstead, M. M.; Balch, A. L. *Inorg. Chem.* **1987**, *26*, 377.
(24) Balch, A. L.; Oram, D. E.; Reedy, P. E., Jr., unpublished results.

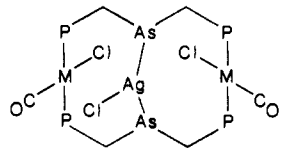

7a, M = Ir
b, M = Rh

However, in these cases, the central silver ion binds the chloride ion and possesses trigonal-planar As_2Cl coordination. The As/Ag–As angles are markedly bent (141.3° in **7a**, 139.5 (1)° in **7b**), and the M···Ag separations (3.36 Å in **7a**, 3.354 (1) and 3.399 (1) Å in **7b**) are much longer than the Ir···Au separations in $[Ir_2AuCl_2(CO)_2(\mu\text{-dpma})_2]^+$. It is important to note that the gold ion in $[Ir_2AuCl_2(CO)_2(\mu\text{-dpma})_5]^+$ shows no tendency to add an additional halide ligand to give a structure like that of **7**.

Crystal and Molecular Structure of $[Ir_2AuCl_4(CO)_2(\mu\text{-dpma})_2]Cl$. The solid consists of one cation and one chloride ion in the asymmetric unit. The atomic positional parameters are given in Table VI. Selected interatomic distances and angles are given in Tables III and IV where they may be compared with those for the gold(I) adduct. Figure 2 shows a perspective drawing of the cation. The anion Cl(5) is clearly separate from this cation. The closest approach between Cl(5) and Au is 6.41 Å.

Although the cation has no symmetry imposed by the crystal symmetry, it does have approximate C_{2v} symmetry, with the twofold axis running through the gold atom and perpendicular to the $AuAs_2Ir_2$ plane. Each iridium has undergone oxidative addition of a gold–chlorine bond. Thus, the coordination environments of both iridium ions are similar with coordination to two trans phosphines, two cis chloride ligands, the terminal carbonyl group, and the gold ion. The gold atom is four-coordinate with bonds to the two iridium atoms and to two arsenic atoms. The Au–Ir distances (2.812 (2), 2.806 (2) Å) are just slightly longer than the general range (2.59–2.72 Å) of Au–Ir bond distances.[16-20]

The differences and similarities of $[Ir_2AuCl_2(CO)_2(\mu\text{-dpma})_2]^+$ and $[Ir_2AuCl_4(CO)_2(\mu\text{-dpma})_2]^+$ are apparent from the parameters in Tables III and IV. Figure 3 compares projections of the center sections of the two cations. The two cations differ by the addition of Cl(3) and Cl(4) to the two iridium atoms. The Au–Ir distances have shortened by 0.22 Å upon oxidation. In contrast, Au–As distances shorten by only an insignificant 0.014 Å. The coordination of the two iridium atoms has undergone reorientation so that the angle between the $IrP_2(CO)Cl$ coordination planes is 168.7°: they are nearly parallel. In contrast, in $[Ir_2AuCl_2(CO)_2(\mu\text{-dpma})_2]^+$ they are inclined at 65.1°. The twisting of the P–Ir and As–Au bonds is much less in $[Ir_2AuCl_4(CO)_2(\mu\text{-dpma})_2]^+$ than in $[Ir_2AuCl_2(CO)_2(\mu\text{-dpma})_2]^+$. This can be seen by comparison of the dihedral angles in Table V. As a consequence of this reduced twist, the $Ir_2(CO)_2Cl_4$ core is more nearly planar than is the $Ir_2(CO)_2Cl_2$ core in $[Ir_2AuCl_2(CO)_2(\mu\text{-dpma})_2]^+$. Likewise, the Ir–Au–Ir angle in the oxidized form is more nearly linear than is the corresponding angle (149.0°) in the reduced complex.

Electronic Absorption and Emission Spectra. The electronic absorption spectrum of $[Ir_2AuCl_2(CO)_2(\mu\text{-dpma})_2]^+$ (**4b**) in dichloromethane solution is shown in the solid line at the top of Figure 4. The spectrum is dominated by an intense absorption at 508 nm. The emission spectrum of this ion obtained from dichloromethane solution at 25° is shown as a dotted line in Figure 4. An intense emission is seen at 605 nm. A excitation spectrum reveals that this emission results from irradiation of the intense low-energy absorption at 508 nm. On the basis of the small Stokes shift observed, we tentatively assign the emission to fluorescence. The electronic absorption spectra of the $[Ir_2AuCl_2(CO)_2(\mu\text{-dpma})_2]^+$ (**4a**) is compared with that of its bromide **4b** and iodide **4c** analogues in the bottom half of Figure 4. The spectral patterns are very similar, with the change in halide producing small shifts to lower energy in the sequence Cl > Br > I. Analogous shifts to lower energy are also observed in the emission spectra of these complexes.

Table III. Selected Interatomic Distances (Å) in $[Ir_2AuCl_2(CO)_2(\mu\text{-dpma})_2]BPh_4$ (**4a**) and $[Ir_2AuCl_4(CO)_2(\mu\text{-dpma})_2]Cl$ (**5a**)

	4a cation	5a cation
	At Ir(1)	
Ir(1)···Au	3.059 (1)	2.812 (2)
Ir(1)–P(1)	2.333 (3)	2.390 (9)
Ir(1)–P(4)	2.312 (4)	2.364 (9)
Ir(1)–C(1)	1.79 (2)	1.88 (3)
Ir(1)–Cl(1)	2.355 (4)	2.400 (7)
Ir(1)–Cl(3)		2.456 (7)
C(1)–O(1)	1.14 (2)	1.11 (4)
	At Ir(2)	
Ir(2)···Au	3.012 (1)	2.806 (2)
Ir(2)–P(2)	2.324 (3)	2.37 (1)
Ir(2)–P(3)	2.317 (3)	2.365 (9)
Ir(2)–C(2)	1.81 (1)	1.77 (3)
Ir(2)–Cl(2)	2.357 (4)	2.395 (7)
Ir(2)–Cl(4)		2.476 (8)
C(2)–O(2)	1.16 (2)	1.21 (3)
	At Au	
Au···Ir(1)	3.059 (1)	2.812 (2)
Au···Ir(2)	3.012 (1)	2.806 (2)
Au–As(1)	2.397 (1)	2.379 (4)
Au–As(2)	2.397 (1)	2.386 (4)

Table IV. Selected Interatomic Angles (deg) in $[Ir_2AuCl_2(CO)_2(\mu\text{-dpma})_2]BPh_4$ (**4a**) and $[Ir_2AuCl_4(CO)_2(\mu\text{-dpma})_2]Cl$ (**5a**)

	4a cation	5a cation
	At Ir(1)	
P(1)–Ir(1)–P(4)	178.4 (1)	164.8 (3)
Cl(1)–Ir(1)–C(1)	172.5 (5)	167 (1)
Au–Ir(1)–Cl(3)		179.6 (2)
P(1)–Ir(1)–Cl(1)	90.6 (1)	85.4 (3)
P(1)–Ir(1)–C(1)	89.8 (5)	97 (1)
P(1)–Ir(1)–Au	84.7 (1)	96.8 (2)
P(1)–Ir(1)–Cl(3)		83.5 (3)
P(4)–Ir(1)–Cl(1)	87.8 (1)	86.5 (3)
P(4)–Ir(1)–C(1)		94 (1)
P(4)–Ir(1)–Au	94.6 (1)	95.0 (2)
P(4)–Ir(1)–Cl(3)		84.6 (3)
Au–Ir(1)–C(1)	115.2 (3)	83 (1)
Au–Ir(1)–Cl(1)	72.1 (1)	83.7 (2)
Cl(3)–Ir(1)–C(1)		97 (1)
Cl(3)–Ir(1)–Cl(1)		96.1 (2)
	At Ir(2)	
P(2)–Ir(2)–P(3)	177.4 (1)	167.4 (3)
Cl(2)–Ir(2)–C(2)	175.1 (5)	166.8 (9)
Au–Ir(2)–Cl(4)		176.3 (2)
P(2)–Ir(2)–Cl(2)	87.4 (1)	88.7 (3)
P(2)–Ir(2)–C(2)	92.8 (4)	92 (1)
P(2)–Ir(2)–Au	96.0 (1)	95.5 (2)
P(2)–Ir(2)–Cl(4)		85.0 (3)
P(3)–Ir(2)–Cl(2)	90.0 (1)	86.5 (3)
P(3)–Ir(2)–C(2)	89.7 (4)	96 (1)
P(3)–Ir(2)–Au	84.0 (1)	95.2 (2)
P(3)–Ir(2)–Cl(4)		83.9 (3)
Au–Ir(2)–C(2)	109.3 (5)	85.8 (9)
Au–Ir(2)–Cl(2)	75.5 (1)	81.0 (2)
Cl(4)–Ir(2)–C(2)		97.9 (9)
Cl(4)–Ir(2)–Cl(2)		95.3 (2)
	At Au	
As(1)–Au–As(2)	173.9 (1)	175.0 (1)
Ir(1)–Au–Ir(2)	149.0 (1)	173.1 (1)
As(1)–Au–Ir(1)	91.6 (1)	87.4 (1)
As(1)–Au–Ir(2)	85.5 (1)	91.7 (1)
As(2)–Au–Ir(1)	87.0 (1)	91.8 (1)
As(2)–Au–Ir(2)	92.7 (1)	89.7 (1)

The electronic absorption spectra of $[Ir_2AuX_4(CO)_2(\mu\text{-dpma})_2]^+$ (X = Cl, Br, I) are shown in Figure 5. The spectrum of the chloro complex is remarkably similar to that of the reduced complex,

Table V. Selected Dihedral Angles (deg)

	4a cation	**5a** cation
P(1)-Ir(1)-Au-As(1)	25.4	16.3
P(4)-Ir(1)-Au-As(2)	20.9	6.9
P(2)-Ir(2)-Au-As(1)	21.1	7.2
P(3)-Ir(2)-Au-As(2)	24.3	12.0
P(1)-Ir(1)-Ir(2)-P(2)	46.1	18.4
P(4)-Ir(1)-Ir(2)-P(3)	44.8	16.5

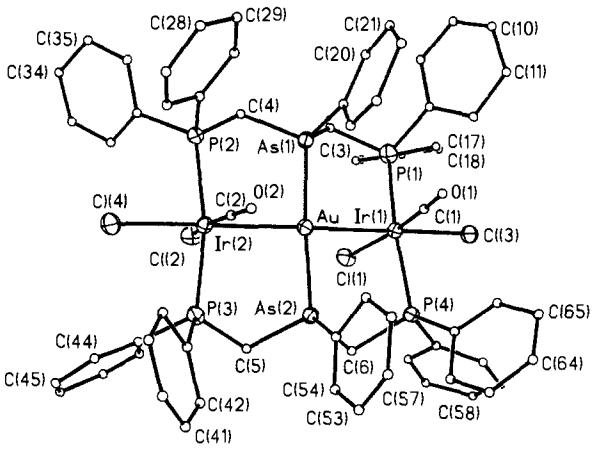

Figure 2. Perspective view of $[Ir_2AuCl_4(CO)_2(\mu\text{-dpma})_2]^+$ (**5a**) using contours as in Figure 1.

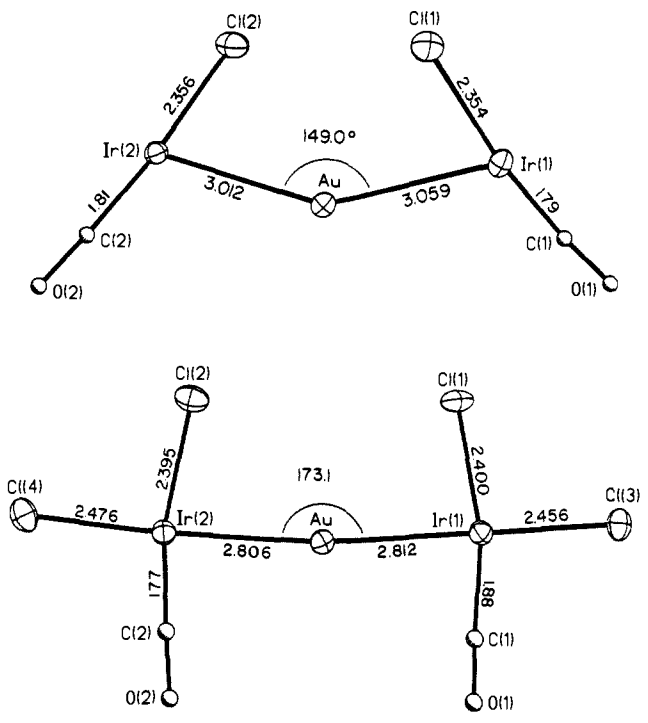

Figure 3. Comparison of the $Ir_2AuCl_n(CO)_2$ cores of $[Ir_2AuCl_2(CO)_2(\mu\text{-dpma})_2]^+$ (**4a**) (top) and $[Ir_2AuCl_4(CO)_2(\mu\text{-dpma})_2]^+$ (**5a**) (bottom).

$(Ir_2AuCl_2(CO)_2(\mu\text{-dpma})_2]^+$, while those of the oxidized bromide and iodide complexes are shifted significantly to lower energies compared to their reduced counterparts and compared to one another. No emission was observed from any of the oxidized complexes. Absorption spectra were also measured for the four mixed-halide complexes, and the λ_{max} values for the lowest energy transitions are shown in Table I. The shift to lower energies seen in the three pure halide complexes is also observed in the mixed-halide complexes. The overall order of energies is $Cl_4 > Cl_2Br_2 > Br_4 > Cl_2I_2 > Br_2I_2 \simeq I_2Br_2 > I_4$. The two isomeric mixed bromide/iodide complexes have nearly identical absorption spectra, indicating that the positions of the bromide and iodide ligands on iridium have little effect on the absorption spectra in the oxidized complexes.

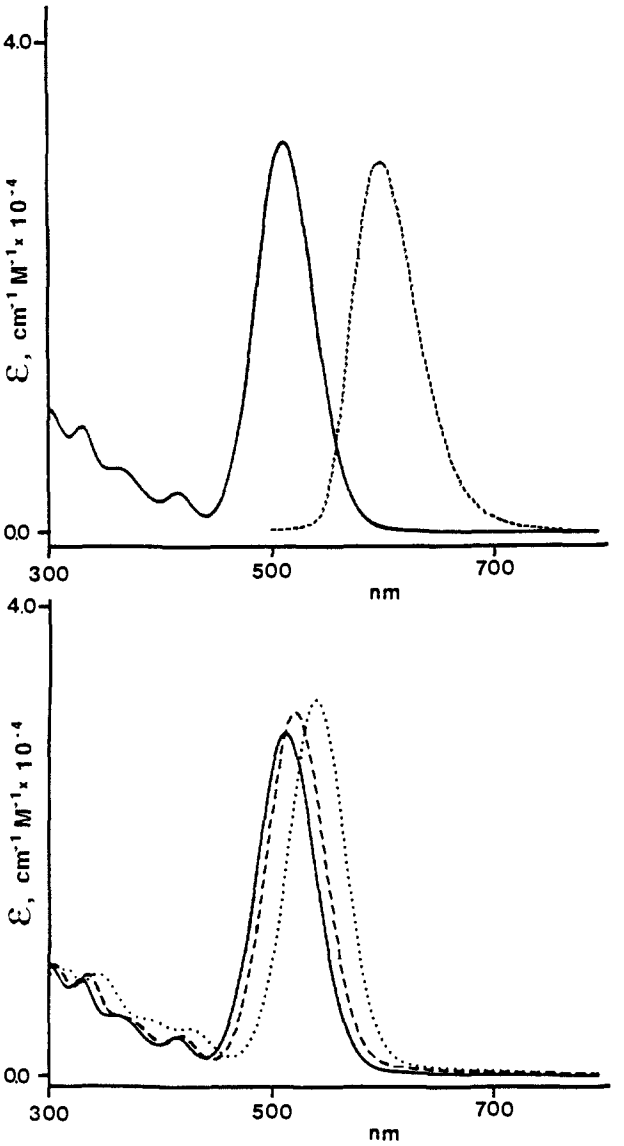

Figure 4. Top: Electronic absorption (solid line) and emission spectra of $[Ir_2AuCl_2(CO)_2(\mu\text{-dpma})_2]^+$ (**4a**) in dichloromethane solution at 25 °C. Bottom: Electronic absorption spectra of $Ir_2AuX_2(CO)_2(\mu\text{-dpma})_2^+$ in dichloromethane. Key: **4a**, X = Cl, solid line; **4b**, X = Br, dashed line; **5c**, X = I, dotted line.

Bonding Model. A qualitative molecular orbital diagram showing the bonding within the Ir···Au···Ir chain in complexes of type **4** is shown in Figure 6. This diagram is limited to showing the essential interactions between the filled d_{z^2} and empty p_z orbitals on gold and iridium. This diagram is closely related to that proposed for $[Rh(CNR)_4]_3^{3+}$.[5] Here, the d^{10} gold center contributes its d_{z^2} and p_z orbitals just as the central rhodium does in $[Rh(CNR)_4]_3^{3+}$, but the d^{10} gold has two less ligands associated with it.

On the basis of this diagram, the intense low-energy transition of **4a** at 508 nm is assigned to a spin-allowed $a_1 \rightarrow b_2$ transition. The luminescence at 605 nm is then assigned as fluorescence resulting from the reverse $b_2 \rightarrow a_1$ process. The observed photochemistry presumably occurs from a so far unobserved triplet state of this $a_1^1b_1^1$ excited state, since the photochemical halogen abstractions seen here are similar to that seen for many d^8–d^8 dimeric complexes where the singlet excited states have been shown to be photochemically inactive.[25,26] A weak maximum at 732

(25) Winkler, J. R.; Marshall, J. L.; Netzel, T. L.; Gray, H. B. *J. Am. Chem. Soc.* **1986**, *108*, 2263.
(26) Steigman, A. E.; Rice, S. F.; Gray, H. B.; Miskowski, V. M. *Inorg. Chem.* **1987**, *26*, 1112.
(27) Dell'Amico, D. B.; Calderazzo, F. *Gazz. Chim. Ital.* **1973**, *103*, 1099.
(28) Charleton, J. S.; Nichols, D. I. *J. Chem. Soc. A* **1970**, 1484.

Table VI. Atomic Coordinates ($\times 10^4$) and Isotropic Thermal Parameters ($Å^2 \times 10^3$) for $[Ir_2AuCl_4(CO)_2(\mu\text{-dpma})_2]Cl$

	x	y	z	U[a]		x	y	z	U[a]
Ir(1)	3054 (1)	6511 (1)	5606 (1)	19 (1)*	C(26)	2981 (22)	8659 (25)	7309 (6)	25 (7)
Ir(2)	1801 (1)	6591 (1)	6747 (1)	19 (1)*	C(27)	3717 (27)	9082 (30)	7503 (9)	45 (10)
Au	2549 (1)	6537 (1)	6193 (1)	19 (1)*	C(28)	4311 (26)	9875 (28)	7428 (7)	37 (9)
As(1)	2541 (2)	8393 (3)	6161 (1)	21 (1)*	C(29)	4167 (24)	10212 (28)	7133 (7)	30 (8)
As(2)	2714 (2)	4684 (3)	6236 (1)	19 (1)*	C(30)	3375 (22)	9771 (26)	6928 (7)	26 (7)
P(1)	2603 (6)	8284 (7)	5483 (2)	26 (3)*	C(31)	565 (23)	9053 (26)	6892 (7)	26 (7)
P(2)	1704 (6)	8435 (8)	6772 (2)	22 (2)*	C(32)	-310 (19)	8582 (25)	6873 (5)	18 (6)
P(3)	1589 (6)	4761 (7)	6780 (2)	22 (3)*	C(33)	-1124 (27)	9136 (29)	6956 (7)	38 (9)
P(4)	3308 (5)	4684 (7)	5594 (2)	19 (3)*	C(34)	-1034 (24)	10142 (26)	7060 (7)	29 (8)
Cl(1)	1287 (5)	6144 (6)	5464 (2)	26 (3)*	C(35)	-56 (24)	10644 (29)	7082 (7)	36 (9)
Cl(2)	224 (5)	6597 (7)	6416 (2)	29 (2)*	C(36)	770 (25)	10094 (27)	7004 (7)	33 (8)
Cl(3)	3493 (5)	6479 (7)	5092 (2)	26 (2)*	C(37)	2425 (21)	4070 (24)	7074 (6)	19 (7)
Cl(4)	1028 (6)	6621 (8)	7217 (2)	30 (3)*	C(38)	2828 (22)	4692 (28)	7344 (6)	26 (7)
Cl(5)	2045 (7)	3480 (8)	1131 (2)	50 (3)*	C(39)	3377 (24)	4146 (27)	7582 (7)	32 (8)
O(1)	5140 (15)	6966 (17)	5923 (4)	29 (5)	C(40)	3576 (27)	3124 (29)	7561 (8)	43 (10)
O(2)	3971 (14)	6606 (19)	7022 (4)	28 (5)	C(41)	3186 (25)	2559 (29)	7315 (7)	37 (9)
C(1)	4368 (25)	6772 (29)	5808 (7)	40 (9)	C(42)	2605 (24)	2999 (27)	7053 (7)	33 (8)
C(2)	3088 (20)	6602 (27)	6913 (6)	24 (6)	C(43)	366 (23)	4301 (26)	6881 (7)	26 (7)
C(3)	1954 (26)	8885 (29)	5768 (7)	36 (9)	C(44)	286 (25)	3989 (27)	7172 (7)	36 (9)
C(4)	1692 (25)	9020 (27)	6413 (7)	28 (8)	C(45)	-526 (21)	3525 (27)	7252 (6)	27 (7)
C(5)	1639 (22)	4093 (24)	6421 (6)	19 (7)	C(46)	-1407 (24)	3374 (31)	7021 (7)	38 (8)
C(6)	2538 (24)	3984 (28)	5857 (7)	31 (8)	C(47)	-1355 (29)	3736 (30)	6714 (8)	47 (10)
C(7)	3589 (23)	9188 (25)	5432 (7)	25 (7)	C(48)	-469 (23)	4107 (25)	6661 (7)	26 (7)
C(8)	3412 (26)	10269 (27)	5425 (7)	33 (8)	C(49)	3976 (21)	4177 (23)	6440 (6)	17 (6)
C(9)	4214 (28)	10962 (33)	5406 (8)	49 (10)	C(50)	4847 (22)	4872 (26)	6484 (6)	24 (7)
C(10)	5132 (28)	10676 (31)	5401 (8)	47 (10)	C(51)	5730 (31)	4413 (34)	6592 (8)	54 (11)
C(11)	5461 (34)	9628 (38)	5416 (9)	65 (12)	C(52)	5822 (25)	3356 (30)	6672 (7)	38 (8)
C(12)	4610 (23)	8818 (26)	5416 (7)	29 (8)	C(53)	4994 (23)	2742 (28)	6630 (7)	29 (8)
C(13)	1683 (21)	8480 (28)	5130 (6)	25 (7)	C(54)	4087 (21)	3151 (22)	6510 (6)	18 (7)
C(14)	692 (21)	8517 (27)	5141 (6)	26 (7)	C(55)	2853 (22)	4055 (24)	5226 (6)	22 (7)
C(15)	56 (31)	8707 (32)	4880 (8)	54 (11)	C(56)	1893 (26)	3807 (27)	5149 (7)	38 (9)
C(16)	371 (29)	8854 (30)	4585 (9)	49 (10)	C(57)	1500 (27)	3279 (30)	4866 (8)	45 (9)
C(17)	1453 (31)	8819 (33)	4598 (10)	58 (12)	C(58)	2247 (26)	2950 (30)	4694 (8)	41 (9)
C(18)	2132 (27)	8697 (28)	4871 (7)	40 (9)	C(59)	3226 (26)	3183 (28)	4783 (8)	40 (9)
C(19)	3868 (22)	8912 (25)	6263 (7)	24 (7)	C(60)	3527 (29)	3666 (30)	5048 (8)	47 (10)
C(20)	4179 (23)	9922 (26)	6165 (7)	28 (8)	C(61)	4598 (19)	4240 (22)	5689 (5)	12 (6)
C(21)	5109 (23)	10269 (28)	6277 (7)	31 (8)	C(62)	4841 (22)	3268 (26)	5838 (6)	26 (7)
C(22)	5859 (28)	9671 (31)	6453 (8)	45 (10)	C(63)	5853 (24)	2981 (29)	5895 (7)	35 (8)
C(23)	5523 (24)	8592 (29)	6550 (7)	36 (8)	C(64)	6611 (23)	3557 (28)	5800 (6)	32 (8)
C(24)	4589 (21)	8292 (27)	6456 (6)	26 (7)	C(65)	6395 (24)	4454 (27)	5640 (7)	32 (8)
C(25)	2755 (22)	8983 (24)	7017 (6)	18 (7)	C(66)	5333 (22)	4784 (26)	5580 (6)	24 (7)

[a] Values denoted by asterisks indicate equivalent isotropic U defined as one-third of the trace of the orthogonalized U_{ij} tensor.

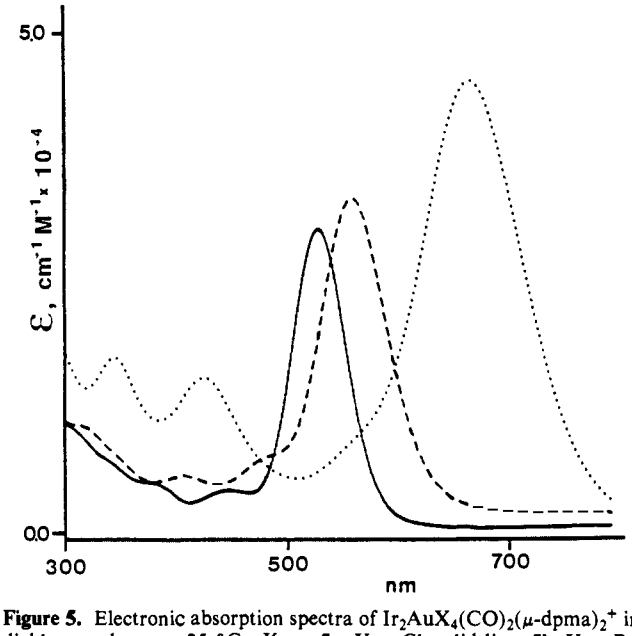

Figure 5. Electronic absorption spectra of $Ir_2AuX_4(CO)_2(\mu\text{-dpma})_2^+$ in dichloromethane at 25 °C. Key: **5a**, X = Cl, solid line; **5b**, X = Br, dashed line; **5c**, X = I, dotted line.

nm in the electronic absorption spectrum of **4a** may correspond to the spin-forbidden component of the 508-nm band.

It is particularly significant that the reactivity of the Au(I) adducts **4** described here is confined to additions to the two vacant coordination sites at the two iridium centers. Despite the low-coordination of the center gold, the chemical reactivity seen so far limits itself to the ends of the $d^8d^{10}d^8$ chain. In general, the behavior of **4** closely parallels that of the $d^8d^8d^8$ chain in **2**.[9] It also should be noted that binuclear d^{10} dimers, particularly $Au_2[(CH_2)PPh_2]_2$, display similar behavior involving transnuclear oxidative addition.[29-31]

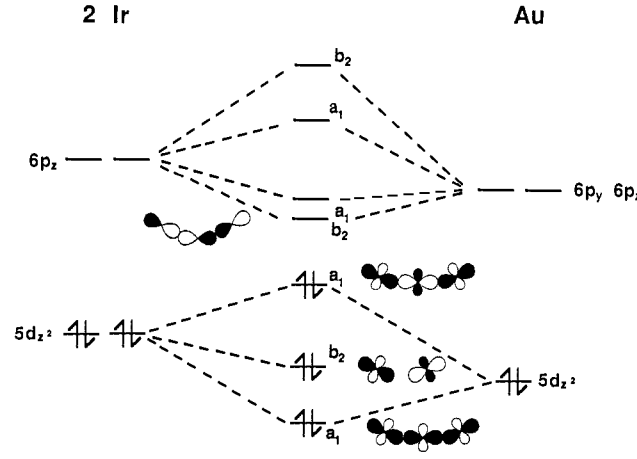

Figure 6. Qualitative molecular orbital diagram illustrating the metal–metal bonding within the Ir–Au–Ir unit. The z axis is taken to be in the Ir–Au–Ir plane and is perpendicular to the twofold axis of rotation centered on Au and bisecting the two Ir atoms. Note that the formal bond order is zero but that $5d_{z^2}$–$6p_z$ mixing through molecular orbitals of the same symmetry results in net stabilization of the Ir–Au–Ir unit.

Experimental Section

Preparation of Compounds. The compounds $Ir_2Cl_2(CO)_2(\mu\text{-dpma})_2$,[10] (CO)AuCl,[27] and $Ph_4AsAuCl_4$[28] were prepared as previously described. Deoxygenated solvents and inert-atmosphere conditions were used in the preparation of $[Ir_2AuCl_2(CO)_2(\mu\text{-dpma})_2]Cl$, while no such precautions were required in the synthesis of $[Ir_2AuCl_4(CO)_2(\mu\text{-dpma})_2]Cl$. The pure complexes are both air-stable as solids and in solution.

$[Ir_2AuCl_2(CO)_2(\mu\text{-dpma})_2]BPh_4$ (4a). A mixture of 100 mg (0.062 mmol) of $Ir_2Cl_2(CO)_2(\mu\text{-dpma})_2$ and 16 mg (0.062 mmol) of (CO)AuCl was placed in a 10-mL flask and cooled to −60 °C. Cold (−60 °C) dichloromethane (5 mL) was added to dissolve the solids. After being stirred for several minutes, the deep red solution was warmed to room temperature. Its volume was reduced to 2 mL under a nitrogen stream. The solution was then filtered and diethyl ether added to precipitate the product as red crystals, yield 100 mg (87%).

$[Ir_2AuCl_2(CO)_2(\mu\text{-dpma})_2]BPh_4$. A solution of 50 mg (0.15 mmol) of sodium tetraphenylborate in 1 mL of methanol was added to a solution of 50 mg (0.027 mmol) of $[Ir_2AuCl_2(CO)_2(\mu\text{-dpma})_2]Cl$ in 2 mL of dichloromethane. After the mixture was stirred for several minutes, methanol was added to precipitate the product as a red solid, yield 40 mg (70%).

$[Ir_2AuCl_4(CO)_2(\mu\text{-dpma})_2]Cl$ (5a). A solution of 44.8 mg (0.062 mmol) of $Ph_4AsAuCl_4$ dissolved in 2 mL of dichloromethane was added to a solution of 100 mg (0.062 mmol) of $Ir_2Cl_2(CO)_2(\mu\text{-dpma})_2$ in 3 mL of dichloromethane. The reaction solution immediately turned bright red in color, and after several minutes of stirring, red needles began to precipitate from the solution. Diethyl ether was added to ensure complete precipitation of the product, yield 95 mg (82%).

$[Ir_2AuBr_2(CO)_2(\mu\text{-dpma})_2]BPh_4$ (4b). A solution of 100 mg (0.97 mmol) of sodium bromide in 2 mL of methanol was added to a solution of 100 mg (0.054 mmol) of $[Ir_2AuCl_2(CO)_2(\mu\text{-dpma})_2]Cl$ in 5 mL of dichloromethane. The slow addition of 5 mL of methanol caused the product to precipitate as the bromide salt. The red crystalline solid was collected by filtration and washed with methanol and diethyl ether. The solid was then redissolved in a solution of 100 mg (0.29 mmol) of sodium tetraphenylborate dissolved in 2 mL of methanol and 4 mL of dichloromethane. The dark red solution was filtered, and 5 mL of methanol was slowly added, which caused the product to precipitate as the tetraphenylborate salt. The red crystalline solid was collected by filtration and washed successively with methanol and diethyl ether; yield 98 mg (82%). Anal. Calcd for $C_{90}H_{78}As_2AuBr_2Ir_2O_2P_4$: C, 48.75; H, 3.55; Br, 7.21. Found: C, 49.21; H, 3.45; Br, 7.50.

$[Ir_2AuI_2(CO)_2(\mu\text{-dpma})_2]BPh_4$ (4c). This complex was prepared by the same procedure used to synthesize **4b**. The methanol solution of sodium bromide was replaced with a solution of 150 mg (1.0 mmol) of sodium iodide in 2 mL of methanol. The product was obtained as purple crystals, yield 105 mg (85%). Anal. Calcd for $C_{90}H_{78}As_2AuBI_2Ir_2O_2P_4$: C, 46.77; H, 3.40; I, 10.98. Found: C, 46.61; H, 3.29; I, 10.99.

$[Ir_2AuBr_4(CO)_2(\mu\text{-dpma})_2]Br$ (5b). A solution of 100 mg (0.045 mmol) of $[Ir_2AuBr_2(CO)_2(\mu\text{-dpma})_2]BPh_4$ in 4 mL of dichloromethane was treated with a solution of 14.9 mg (0.045 mmol) of carbon tetrabromide dissolved in 1 mL of dichloromethane. The initially red solution turned immediately purple in color. Addition of diethyl ether caused a purple solid to precipitate. The product was collected by filtration and washed with diethyl ether; yield 80 mg (75%). Anal. Calcd for $C_{66}H_{58}AuAs_2Br_5Ir_2O_2P_4$: C, 37.08; H, 2.73; Br, 18.69. Found: C, 35.97; H, 2.55; Br, 20.5.

$[Ir_2AuI_4(CO)_2(\mu\text{-dpma})_2]BPh_4$ (5c). A solution of 100 mg (0.043 mmol) of $[Ir_2AuI_2(CO)_2(\mu\text{-dpma})_2]BPh_4$ in 4 mL of dichloromethane was treated with either 10.9 mg (0.043 mmol) of diiodine or 22.3 mg (0.043 mmol) of carbon tetraiodide dissolved in 1 mL of dichloromethane. In each case, the initially red solution turned immediately dark green in color. The addition of diethyl ether caused green crystals to precipitate. The product was collected by filtration and washed with diethyl ether; yield 97 mg (87%).

$[Rh_2AuCl_2(CO)_2(\mu\text{-dpma})_2]BPh_4$ (6). A mixture of 100 mg (0.07 mmol) of $Rh_2Cl_2(CO)_2(\mu\text{-dpma})_2$ and 18.2 mg (0.07 mmol) of ClAu(CO) was placed in a 10-mL flask and cooled to −60 °C under a dry nitrogen atmosphere. The solids were dissolved in 4 mL of cold (−60 °C) dichloromethane and the resulting orange solution stirred for 10 min. The solution was then warmed to room temperature and ether added to precipitate the product as the chloride salt. The orange crystalline solid was collected by filtration, washed with diethyl ether, and then redissolved in a minimum amount of dichloromethane. Addition of a solution of 100 mg (0.29 mmol) of sodium tetraphenylborate in 2 mL of methanol precipitated the product as the tetraphenylborate salt. The orange crystalline solid was collected by filtration and washed successively with methanol and diethyl ether; yield 95 mg (70%). Anal. Calcd for $C_{90}H_{78}As_2AuBCl_2O_2P_4Rh_2$: C, 55.44; H, 4.03; Cl, 3.64. Found: C, 56.17; H, 3.99; Cl, 3.86.

(29) Schmidbaur, H. *Acc. Chem. Res.* **1975**, *8*, 62.
(30) Fackler, J. P., Jr.; Basil, J. D. *Organometallics* **1982**, *1*, 871.
(31) Murray, H. H.; Fackler, J. P., Jr. *Inorg. Chim. Acta* **1986**, *115*, 207.

Table VII. Crystal Data and Data Collection Parameters

	$[Ir_2AuCl_2(CO)_2(dpma)_2]$-$BPh_4{\cdot}CH_2Cl_2$	$[Ir_2AuCl_4(CO)_2(dpma)_2]Cl$
formula	$C_{91}H_{80}As_2AuBCl_4Ir_2O_2P_4$	$C_{66}H_{58}As_2AuCl_5Ir_2O_2P_4$
fw	2213.21	1915.42
cryst syst	monoclinic	monoclinic
space gp	$P2_1/n$	$P2_1/c$
a, Å	13.677 (6)	13.346 (5)
b, Å	22.407 (6)	12.794 (3)
c, Å	27.143 (9)	44.824 (30)
β, deg	93.15 (3)	98.29 (4)
V, Å^3	8306 (3)	7573 (6)
Z	4	4
d_{calcd}(130 K), g·cm^{-3}	1.77	1.67
cryst dimens, mm	0.20 × 0.30 × 0.37	0.15 × 0.17 × 0.20
diffractometer	Syntex $P2_1$	Syntex $P2_1$
radiatn (graphite monochromated)	Mo Kα (λ = 0.71069 Å)	Mo Kα (λ = 0.71069 Å)
μ(Mo Kα), cm^{-1}	62.8	69.1
temp, K	130	130
range of transmissn factors	0.179–0.364	0.299–0.429
$2\theta_{max}$, deg	50	50
scan type	ω	ω
scan speed, deg·min^{-1}	30	15
scan range, deg	0.9	1.0
w bkgd offset, deg	0.8	1.0
octants collected	$+h,+k,\pm l$	$+h,+k,\pm l$
R(MERGE)	0.090	0.036
no. of unique data	14622	6804
no. of unique data used	9359 [$F_o > 6\sigma(F_o)$]	5255 [$F_o > 6\sigma(F_o)$]
no. parameters refined	482	399
check reflcn interval no.	2 measd every 200 reflcns	2 measd every 200 reflcns
R	0.050	0.067
R_w	0.059	0.075

X-ray Data Collection. $[Ir_2AuCl_2(CO)_2(\mu\text{-dpma})_2]BPh_4{\cdot}CH_2Cl_2$ (4a). Red-green dichroic crystals were formed by slow diffusion of a methanol solution of sodium tetraphenylborate into a dichloromethane solution of $[Ir_2Au(\mu\text{-dpma})_2(CO)_2Cl_2]Cl$. The crystals were removed from the diffusion tube and rapidly coated with a light hydrocarbon oil to reduce loss of solvent from the crystal. The crystal was mounted in the cold stream of a Syntex $P2_1$ diffractometer equipped with a modified LT-1 low-temperature apparatus. Unit cell parameters were obtained from a least-square refinement of 10 reflections with $13 \le 2\theta < 25°$. The space group $P2_1/n$ (an alternate of $P2_1/c$) was uniquely determined by the observed conditions: $h0l$, $h + l = 2n$; $0k0$, $k = 2n$. No decay in the intensities of two standard reflections occurred. Data collection parameters are summarized in Table VII. The data were corrected for Lorentz and polarization effects.

$[Ir_2AuCl_4(CO)_2(\mu\text{-dpma})_2]Cl$ (5a). Red parallelepipeds were formed by slow diffusion of diethyl ether into a dichloromethane solution of the compound. Unit cell parameters were obtained from a least-squares refinement of 10 reflections with $15 \le 2\theta \le 25°$. The space group $P2_1/c$ (No. 14) was uniquely determined by the observed conditions: $h0l$, $l = 2n$; $0k0$, $k = 2n$. No decay in the intensities of two standard reflections occurred. Data collection parameters are summarized in Table VII. All other data collection procedures were identical with those of **4a**.

Solution and Refinement of Structures. $[Ir_2AuCl_2(CO)_2(\mu\text{-dpma})_2]$-$BPh_4{\cdot}CH_2Cl_2$ (4a). All structure determination calculations were done on a Data General Eclipse MV/10000 computer using the SHELXTL Version 4 software package. The positions of the two iridium atoms and the gold atom were generated from FMAP8, the Patterson-solving routine of SHELXTL. Other atom positions were located from successive difference Fourier maps. Anisotropic thermal parameters were assigned to the elements iridium, gold, phosphorus, and arsenic. Anisotropic thermal parameters were also assigned to each of the chloride atoms

bonded to the two iridium atoms. Isotropic thermal parameters were used for all other atoms. All hydrogen atoms were fixed at calculated positions by using a riding model in which the C-H vector is fixed at 0.96 Å and the isotropic thermal parameter for each hydrogen atom is given a value 20% greater than the carbon atom to which it is bonded. Scattering factors and corrections for anomalous dispersion were taken from a standard source.[32] The final stages of refinement included an absorption correction.[33] The final R value of 0.050 was computed with a data to parameter ratio of 19.4. This yielded goodness-of-fit of 0.684 and a mean shift/esd of 0.015 for overall scale on the last cycle of refinement. A value of 3.0 e/Å^3 was found as the largest feature on the final difference Fourier map. This peak was located 0.78 Å from a chlorine atom in a disordered dichloromethane molecule. Due to the well-behaved thermal parameters of this molecule, no attempt was made to model the disorder. The weighting scheme used was $w = [\sigma^2(F_o)]^{-1}$. Corrections for anomalous dispersion were applied to all atoms.

$[Ir_2AuCl_4(CO)_2(\mu\text{-dpma})_2]Cl$ (**5a**). The positions of the two iridium atoms and the gold atom were generated from FMAP8. Other atoms positions were located from successive difference Fourier maps. Anisotropic thermal parameters were assigned to the elements iridium, gold, arsenic, phosphorus, and chloride while isotropic thermal parameters were used for the remaining atoms. The final stages of refinement included an absorption correction and the treatment of all hydrogen atoms as described for **4a**. The final R value of 0.067 was computed with a data to parameter ratio of 13.2. This yielded a goodness-of-fit of 1.287 and a mean shift/esd of 0.013 for overall scale on the last cycle of refinement. A value of 1.70 e/Å^3 was found as the largest feature on the final difference Fourier map. This peak was located 0.80 Å from Cl(5). The weighting scheme used was $w = [\sigma_2(F_o)]^{-1}$.

(32) *International Tables for X-ray Crystallography*; Kynoch: Birmingham, England, 1974; Vol. 4.

(33) The method obtains an empirical absorption tensor form an expression relating F_o and F_c: Hope, H.; Moezzi, B. *Program XABS*; Department of Chemistry, University of California: Davis, CA.

Acknowledgment. We thank the National Science Foundation (Grant CHE8519557) for support, Bowdoin College for faculty study leave for J.K.N., Dow Corning Corp. for a fellowship for P.E.R., the Earl C. Anthony Fund for a fellowship to D.E.O., and Johnson Matthey Inc. for a loan of iridium.

Supplementary Material Available: Tables of bond distances, bond angles, anisotropic thermal parameters, and hydrogen atom positions for **4a** and **5b** (13 pages); listings of observed and calculated structure factors (82 pages). Ordering information is given on any current masthead page.

Chemistry of Dibenzo[2.2]paracyclophane and Its Related Compounds. Evidence for the Existence of a Cyclophyne Intermediate[1]

Chin Wing Chan and Henry N. C. Wong*[2]

Contribution from the Department of Chemistry, The Chinese University of Hong Kong, Shatin, New Territories, Hong Kong. *Received May 29, 1987*

Abstract: The syntheses of dibenzo[2.2]paracyclophane (**5**), benzonaphtho[2.2]paracyclophane (**6**), benzofurano[*c*][2.2]-paracyclophane (**7**) and 1,2,3-selenadiazolobenzo[2.2]paracyclophane (**28**) are presented. The existence of the strained cyclophyne **10** as an intermediate was established by a trapping method. Benzofurano[*c*][2.2]paracyclophane (**7**) serves as a diene in the Diels-Alder reaction as illustrated by the preparation of the ester **34**. The preparation of a macroparacyclophane diacetylene **36** is described. The electronic spectra of some of the cyclophanes are discussed.

Cyclophanes belong to one of the remarkable compound classes that has attracted extensive studies.[3] In the domain of organic synthesis, preparation of the alkenes **1** and **2** (Chart I) pioneered the study of classically conjugated but orbitally unconjugated compounds.[4] The C-C double bonds in **1** and **2** are orthogonal to the central rings, because rotation of the benzene moiety is restricted by its large steric demand.

The introduction of aromatic rings orthogonal to the central benzenes in **1** and **2** has also attracted considerable attention. The rigid molecular frameworks of **3** and **4** provide fixed geometry for orthogonal benzenes.[5] We report here the synthesis of dibenzo[2.2]paracyclophane (**5**), benzonaphtho[2.2]paracyclophane (**6**), benzofuran[*c*][2.2]paracyclophane (**7**) as well as 1-methyldibenzo[2.2]paracyclophane (**8**) (Chart II). The *gem*-dibromide **9** will serve as the starting material. The detection of the existence of intermediate **10** in our synthesis is made possible by trapping

Chart I

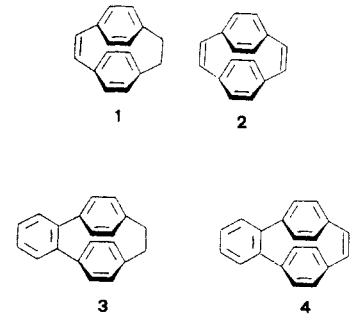

(1) Arene Synthesis by Extrusion Reaction. 12. Part 11: Wong, H. N. C.; Man, Y.-M.; Mak, T. C. W. *Tetrahedron Lett.*, in press. Taken in part from: Chan, C. W. M. Phil. Thesis, The Chinese University of Hong Kong, 1987. A preliminary account of this work has appeared. See: Chan, C. W.; Wong, H. N. C. *J. Am. Chem. Soc.* **1985**, *107*, 4790-4791.

(2) Also known as Nai Zheng Huang.

(3) For reviews, see: Vögtle, F.; Neumann, P. *Top. Curr. Chem.* **1971**, *48*, 67-129. Vögtle, F.; Hohner, G. *Top. Curr. Chem.* **1978**, *74*, 1-29. Boekelheide, V. *Top. Curr. Chem.* **1983**, *113*, 87-143. Vögtle, F.; Rossa, L. *Angew. Chem., Int. Ed. Engl.* **1979**, *18*, 515-529. Kleinschroth, J.; Hopf, H. *Angew. Chem., Int. Ed. Engl.* **1982**, *21*, 469-480. Keehn, P. M.; Rosenfeld, S. M. *Cyclophanes*; Academic: New York, 1983; Vols. I, II.

(4) Dewhirst, K. C.; Cram, D. J. *J. Am. Chem. Soc.* **1958**, *80*, 3115-3125; *J. Am. Chem. Soc.* **1959**, *81*, 5963-5971.

(5) Jacobson, N.; Boekelheide, V. *Angew. Chem., Int. Ed. Engl.* **1978**, *17*, 46-47.

0002-7863/88/1510-0462$01.50/0